



# DEM spatial resolution sensitivity in the calculation of the RUSLE LS-Factor and its implications in the estimation of soil erosion rates in Ecuadorian basins

Daniel Delgado<sup>1,2</sup> · Mahrez Sadaoui<sup>1</sup> · Wolfgang Ludwig<sup>1</sup> · Williams Méndez<sup>2,3</sup>

Received: 10 March 2023 / Accepted: 22 November 2023 / Published online: 27 December 2023  
© The Author(s), under exclusive licence to Springer-Verlag GmbH Germany, part of Springer Nature 2023

## Abstract

The length and steepness of the slope (LS-Factor) describe the role that topography plays in the hazard of soil erosion and constitutes one of the five factors that allow the determination of soil loss using the Revised Universal Soil Loss Equation (RUSLE) mathematical model. This factor is calculated using Digital Elevation Models (DEM); however, its spatial scale may affect the quality of its estimation. The objective of the present investigation was to analyze the sensitivity of the DEM spatial resolution in the calculation of RUSLE LS-Factor and to determine its implications in the estimation of soil erosion rates in Ecuadorian basins. The methodology considered the delimitation of the hydrographic basins and the evaluation of data from SRTM, HydroSHEDS and ALOS PALSAR as providers of DEMs databases through the implementation of two statistical methods. The delimitation of the basins was obtained from the regional literature and the DEMs databases from web servers. Comparisons of the results at the national scale and at the basin scale were established using the original spatial scales and a common scaling of 1 and 4 km. The results will make it possible to determine the most appropriate spatial scale of DEM database to determine soil erosion rates considering the particular conditions of the study area, applying the RUSLE model.

**Keywords** Slope · Revised universal soil loss equation · GIS · Andisols · Ecuador

## Introduction

Soil loss is one of the main environmental problems that threatens all terrestrial ecosystems and its negative effects are increasingly worrying due to climate change (Montanarella et al. 2015; Borrelli et al. 2017). Global annual soil

loss is estimated at 75 billion tons, generating an approximate cost of 400 billion dollars (USD) annually, with rates of around 16 t/ha/year in the United States, out of 10 to 20 t/ha/year in Europe and between 20 and 40 t/ha/year in Asia, Africa, and South America (Melkam 2003), which makes this problem a great threat to global agricultural production (Li et al. 2022). Despite this problem, South America is the region of the world with the fewest number of studies related to soil loss, with only 123 case-studies, considering the 976 applied in Asia or the 929 applied in Europe (Borrelli et al. 2021). In Ecuador, significant efforts have been made to estimate soil erosion due to rainfall. Research at localities on the coast (Pacheco et al. 2019; Mendoza et al. 2023; Párraga et al. 2023; Véliz et al. 2023), Andes (Harden 1988, 2001; De Noni et al. 2000; Molina et al. 2007; Vanacker et al. 2007, 2022; Ochoa-Cueva et al. 2015), or at national scale (Delgado et al. 2021, 2022, 2023) have determined erosion rates or provided important inputs for their estimation. However, these investigations have not been sufficient to cover the entire national problem. This generates a lack of understanding

✉ Daniel Delgado  
daniel.delgado@utm.edu.ec

<sup>1</sup> Centre de Formation et de Recherche sur les Environnements Méditerranéens, Université de Perpignan, Via Domitia, UMR 5110, 52 Avenue Paul Alduy, 66860 Perpignan CEDEX, France

<sup>2</sup> Departamento de Construcciones Civiles y Arquitectura, Facultad de Ciencias Matemáticas, Físicas y Químicas, Universidad Técnica de Manabí, Avenida José María Urbina, Portoviejo EC130105, Manabí, Ecuador

<sup>3</sup> Centro de Investigación Estudios del Medio Físico Venezolano, Instituto Pedagógico de Caracas, Universidad Pedagógica Experimental Libertador, Venezuela University, El Paraíso 1020, Distrito Capital, Caracas, Venezuela

of the real consequences that this phenomenon can cause in terms of ecological imbalance, loss of habitat, interruption of life cycles, and reduction of natural traps for CO<sub>2</sub> capture, among others.

Soil erosion analysis involves many factors, such as climatic and human-induced, as well as topographical factors (Panagos et al. 2021) and topsoil characteristics (physical and chemical properties that determine its erodibility, Delgado et al. 2023). The length factor (L) and the slope factor (S) are dimensionless topographic factors, with values equal to or greater than 0, which are analyzed together and represented with the LS symbology, determining higher erosion rates when their values are higher (Senanayake et al. 2022).

RUSLE model is one of the main tools to determine the characteristics of soil erosion worldwide, with results validated in numerous investigations (Renard et al. 1991; Thomas et al. 2018; Batista et al. 2019). The RUSLE factors include: (1) R-Factor (rainfall erosivity, main generator of soil water erosion; Delgado et al. 2022); (2) K-Factor (soil erodibility); (3) (4) LS-Factor (topographic factor that combines the length and inclination of the slope); (5) C-Factor (land use and cover); and (6) P-Factor (soil conservation practices).

The use of data from remote sensors and geographic information systems allows the determination of complex terrain characteristics that are even inaccessible in the area and have proven to be suitable for the RUSLE model (Elnashar et al. 2021). For the use of these geomatics tools applied to geospatial analysis, a good digital cartography is required, whose most useful raster format is represented by DEM. These are a quantitative representation of the land surface, and provides information about the terrain, allowing attributes, such as slope, area and drainage network, curvature, among others parameters (Mukherjee et al. 2014).

In this way, to calculate the LS-Factor, it is enough to apply models that use satellite raster information. However, the DEM spatial resolution to be used will play a fundamental role in the quality of the estimation of the results of these factors (Panagos et al. 2015). Molnar and Julien (1998) concluded that the grid size mainly affects the S-Factor, since the slope becomes smoother as the cell resolution decreases.

The main objective of the present investigation was to analyze the sensitivity of the DEM spatial resolution in the calculation of the RUSLE LS-Factor and to determine its implications in the estimation of soil erosion rates in the Ecuadorian basins, both for the basins that drain to the Pacific (Ecuadorian Coastal Basins—ECB) and those that drain to the Amazon (Amazon Tributaries Basins—ATB).

The results of this research will improve the estimates of erosion rates in the Ecuadorian basins using the RUSLE model, obtaining better planning to determine priority areas of attention that require particular soil management plans and conservation measures to cushion or slow soil erosion

by rainfall through the analysis of the LS-Factor, a methodology that can be applied in other sectors worldwide.

## Study area

The study area includes the continental territory of Ecuador, in South America, located within latitudes 5.04°S–1.48°N and longitudes 81.03°W–75.16°W. It limits to the North with Colombia, to the South and to the East with Peru, and to the West with the Pacific Ocean.

The Ecuadorian territory was classified into 32 basins according to the procedure carried out in the investigation by Delgado et al., (2021), of which 24 are located to the West and are called ECBs, because they discharge into the Pacific Ocean, while the remaining 8, located to the East, are called ATBs and discharge into the Amazon (Fig. 1). Within the ECBs, three basins stand out which, despite continuing to discharge into the Pacific Ocean, do so outside the national territory (Id 1 to Colombia; Id 23 and 24 to Peru in Fig. 1).

The condition for the distribution of the basins was through their extension, choosing those with areas greater than 500 km<sup>2</sup>, which covers more than 227,000 km<sup>2</sup> and represents almost 80% of the continental national territory. In general, both groups of basins have very different and irregular characteristics, where the ATBs stand out for



**Fig. 1** Study area and basins distribution in Ecuadorian territory. Yellow (21) and pink (3) color represent ECBs and green (8) color represent ATBs

their greater extension and greater presence of precipitations (Delgado et al. 2022).

## Methodology

### DEM HydroSHEDS

HydroSHEDS is a database containing raster and vector layers that describe the topography, drainage networks, and watersheds of the Earth's surface at a spatial scale of 30 arc-sec ( $\approx 1$  km) (Lehner et al. 2008). The primary data source used in the development of HydroSHEDS was the SRTM digital elevation model at a resolution of 3 arc-seconds ( $\sim 90$  m at the equator, with some custom-modifications, as the filling of sinks that would have an effect on the smoothing of slopes), which is supported by auxiliary sources, including SRTM water body information (<http://edc.usgs.gov/products/elevation/swbdguide.doc>), river data from the Digital Chart of the World (DCW) (ESRI, 1992; ESRI, 1993), and the Global Lakes and Wetlands Database (EROS 2017).

We proceeded to download the DEM for the entire Ecuadorian territory and later adapt it to the study area, homogenize the projection (WGS84-UTM zone 17S) and spatial resolution (1 km) using Software R. The DEM was also converted to a spatial resolution of 4 km to compare the results shown by Delgado et al., (2021) with the other DEM databases and determine the incidence of a coarser scaling in the LS-Factor values.

### DEM shuttle radar topographic mission (SRTM)

SRTM is an international project of the National Aeronautics and Space Administration (NASA) and the National Geospatial-Intelligence Agency (NGA) to acquire radar data that was used to generate maps of near global elevations.

To cover the entire Ecuadorian territory, 34 mosaics of  $\approx 110$  km<sup>2</sup> of area (not correspond to the pixel size) were downloaded from the SRTM 1 Arc-Second Global database (EROS, 2017) using the QGIS SRTM-Downloader plugins. SRTM provides near-complete world data coverage at an initial spatial resolution of 1 arc-sec ( $\approx 30$  m). Subsequently, using R Software, the study area was cut out, and the projection (WGS84-UTM zone 17S) and spatial resolution (30 m) were homogenized. The DEM was also modified to a spatial resolution of 1 km and 4 km to compare the changes generated by the scaling process with the other DEM databases considered in the present investigation.

### DEM ALOS PALSAR

ALOS Phased Array type L-band Synthetic Aperture Radar (ALOS PALSAR) is a space mission carried out from 2006 to 2011, which obtained detailed observations of the earth's surface day and night in all weather conditions. The values obtained by PALSAR contain two fine beam modes: single polarization (FBS) and dual polarization (FDB). These two modes provide information with very fine spatial resolutions, starting from 10 m (FBS) to 20 m (FDB). However, the program does not allow generating DEMs of the entire earth's surface. In Ecuador, these restrictions are also present, so the database will be applied to evaluate only one study basin (ECB Portoviejo, ID 9 in Fig. 1) and compare it with the results obtained from the two previous DEMs databases, without being able to consider the entire Ecuadorian territory. For this, the projection (WGS84-UTM zone 17S) and spatial resolution (12.5 m) were homogenized. DEM was also modified to a spatial resolution of 4 km to compare the changes generated by the scaling process with the other DEMs databases considered in the present investigation.

### Slope length (L) and slope steepness (S) factor calculation (LS-Factor)

#### L-Factor calculation

The L-Factor was calculated using the model proposed by Desmet & Govers (1996) (Eqs. 1, 2 and 3):

$$L_{(i,j)} = \frac{[A_{(i,j)} + D^2]^{(m+1)} - A_{(i,j)}^{(m+1)}}{x_{(i,j)}^m D^{(m+2)} (22.13)^m}, \quad (1)$$

where  $A_{(i,j)}$ : contributing area at the inlet of grid cell with coordinates  $(i,j)$  measured in m<sup>2</sup>,  $D$ : grid cell size (m),  $X_{(i,j)}$ :  $(\sin \alpha_{i,j} + \cos \alpha_{i,j})$  the aspect direction of the grid cell with coordinates  $(i,j)$  (being a pixel the value is  $x=1$ ).  $\alpha_{i,j}$ : aspect direction for the grid cell with coordinates  $(i,j)$ .  $m$ : related to the ratio  $\beta$  of the rill to interrill erosion:

$$m = \frac{\beta}{1 + \beta}, \quad (2)$$

where

$$\beta = \frac{\sin \theta / 0.0896}{3(\sin \theta)^{0.8} + 0.56}, \quad (3)$$

$\beta$  = slope direction.

$\theta$  = slope at the pixel level.

To calculate the L-Factor, it is necessary to apply a flow direction algorithm. Grass GIS software Watershed algorithm was used for each of the DEMs databases, estimating the geometry of the surface network that simulates runoff,

allowing obtaining flow accumulation raster, drainage direction, river location, and basins (Delgado et al. 2021). Previously, DEMs files were fixed using Fill sink option from SAGA group in QGIS.

### S-Factor calculation

The calculation of the S-Factor was carried out using the RUSLE approach of Renard et al., (1996) based on McCool et al., (1987). This methodology considers different equations for two ranges of slopes.  $S_{slow}$  are slopes less than  $5.1^\circ$  ( $\tan \theta < 0.09$  rad) and  $S_{steep}$  are slopes equal to or greater than  $5.1^\circ$  ( $\tan \theta \geq 0.09$  rad).  $\theta$  is the slope in degrees (Eqs. 4 and 5):

$$S_{slow} = 10.8 \sin \theta + 0.03 \quad (4)$$

$$S_{steep} = 16.8 \sin \theta - 0.5. \quad (5)$$

The slope rasters were generated from the DEMs of each database, using the "slope" tool of the QGIS software.

### LS-Factor calculation

Once the L-Factor and S-Factor rasters have been obtained separately, Eq. 6 was used using the R software:

$$LS = L * S, \quad (6)$$

where:  $LS$ : slope length ( $L$ ) and slope steepness ( $S$ ) factor.  $L$ : slope length factor (L-Factor).  $S$ : slope steepness factor (S-Factor).

For LS-Factor calculations with different scales from the original, we initially proceeded to scale the original DEMs to the spatial resolution to be worked on (1 km or 4 km, depending on the database) and then apply the corresponding equations (Eqs. 1, 2, 3, 4, 5 and 6).

### Evaluation of DEMs databases

After LS-Factor calculating through different DEMs databases that had nationwide extension, two standard comparison metrics were used to evaluate their conditions from a statistical approach: Pearson Correlation Coefficient (PCC, Eq. 7) and Root Mean Square Error (RMSE, Eq. 8):

$$PCC = \frac{\text{cov}(LS - \text{Factor}^{SRTM}, LS - \text{Factor}^{HydroSHEDS})}{\sqrt{\text{var}(LS - \text{Factor}^{SRTM})} \sqrt{\text{var}(LS - \text{Factor}^{HydroSHEDS})}} \quad (7)$$

$$RMSE = \sqrt{\frac{1}{N} \sum_{i=1}^n (Y_{iSRTM} - Y_{iHydroSHEDS})^2} \quad (8)$$

where  $LS\text{-Factor}^{SRTM}$  and  $LS\text{-Factor}^{HydroSHEDS}$  are the results obtained from the LS-Factor from these databases;  $n$  is the number of data sets and  $Y_i$  are the LS-Factor values for each method. Equation 7 made it possible to determine the level of linear agreement between both satellite databases, while Eq. 8 evaluated the typical magnitude of the error product of the satellite data and the possibility of outliers.

## Results and discussion

### Influence of DEMs spatial resolution in LS-Factor at national scale

Through the L-Factor HydroSHEDS analysis, higher values were identified at the 4 km scale (between 1 and 28.08, Fig. 2a) in relation to their original scale (between 1 and 15.12, Fig. 2b), but their spatial distribution maintained the same trend. When observing the L-Factor RSTM at its original (Fig. 2e) and modified (Fig. 2f) scale, no clear trend is observed between its spatial distributions. Using a finer scale, each pixel showed different L-Factor values, despite sharing the same area; while, at a coarser scale, zonal values were more homogeneous. With a resolution of 30 m (Fig. 2e) wider ranges of values were recorded, between 1 and 3000, but the data cloud was consolidated between 1 and 12 (indicating that higher values existed, but their frequency was relatively low), highlighting an average value of 3. With a resolution of 4 km (Fig. 2f), both the numerical ranges and spatial distribution were similar to L-Factor HydroSHEDS at its same resolution (Fig. 2b) (between 1 and 29.05), including their mean values (5.88 for HydroSHEDS and 6.23 for SRTM).

When analyzing S-Factor HydroSHEDS (Fig. 2c and 2d) and SRTM (Fig. 2g, h), highest values were recorded in highest areas, according to slopes distribution. In coarser scales (1 km and 4 km), highest values are in Andes Mountains. At a finer scale (30 m), S-Factor was distributed with greater detail and precision, highlighting the appearance of high values in ECBs sectors close to Pacific Ocean and that fit with the existence of small mountain that develop along the Ecuadorian coast, such as Mache-Chindul, Jama, Chongon-Colonche, Balzar, Convento and Cojimies (Reyes 2013). In S-Factor, coarser resolutions generated lower values (unlike Factor-L). HydroSHEDS values ranged from 0.93 to 8.22 for 1 km and from 0.03 to 3.65 for 4 km, while for SRTM values between 0.06 and 16.30 were recorded in 30 m and between 0.03 and 3.91 for 4 km.

L-factor values increased with increasing spatial scale (coarser resolution). Therefore, a DEM scaled to a coarser resolution generalizes the pixel irregularities resulting from the interpolation process, simulating larger sinks that allow for greater flow accumulation. On the contrary, a better

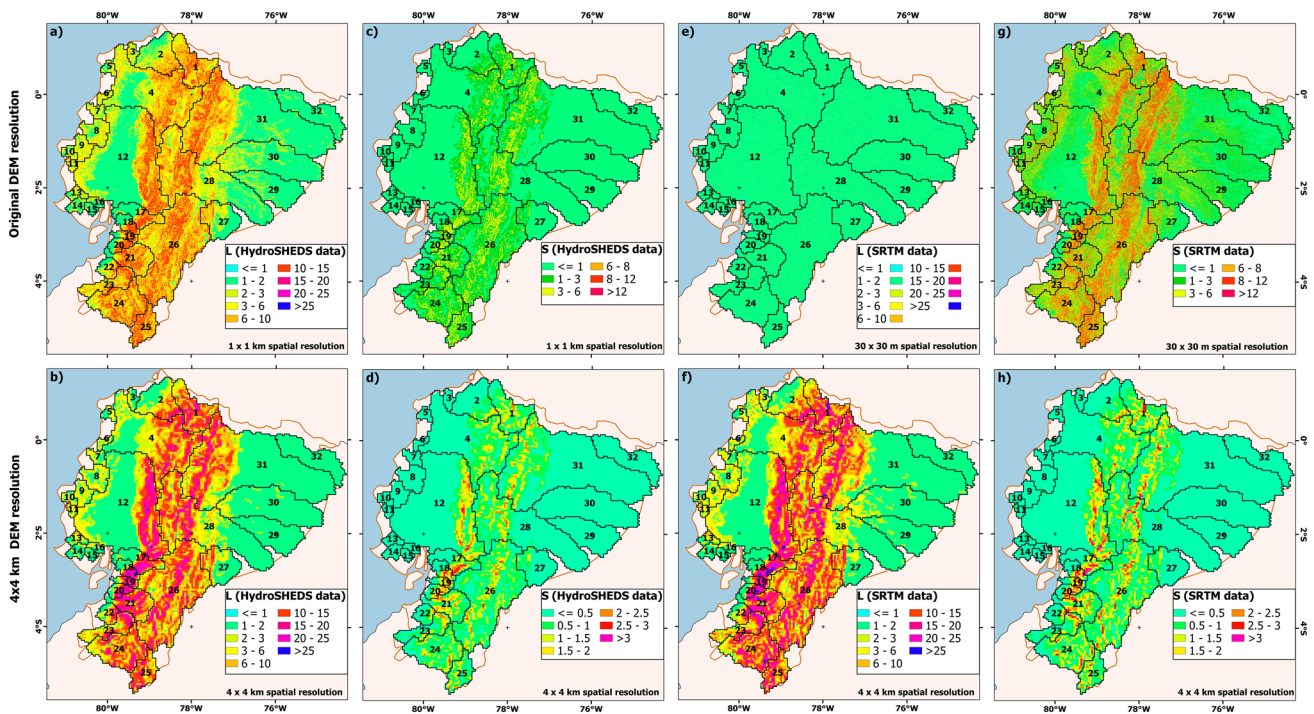


**Fig. 2** L-Factor and S-Factor results for HydroSHEDS (a, b, c and d) and SRTM (e, f, g and h) databases. Spatial resolution details are seen to the left of each row

original DEM resolution characterizes the irregularities and reliefs of the terrain with greater precision, obtaining a much more real flow accumulation.

In contrast, in S-Factor, increase in spatial resolution caused a considerable decrease in its values. On this occasion, the scaling process caused a loss of terrain elevation details, underestimating the large height differences that occur spatially in Andes Mountains and its surroundings, homogenizing their values. Therefore, the scaling process at coarser resolutions masks the real terrain situation, obtaining more spatially biased values in sectors with steepest slope.

Through Fig. 3 it can be identified that both L-Factor and S-Factor had special characteristics that impact on the LS-Factor (addressed in the analysis of Fig. 2). In general, areas with steeper slopes registered highest LS-Factor values, which shows that the gradient of the slope is the factor with the greatest influence on their results.

The scaling process generated that both factors had greater modifications in the highest slopes. A finer resolution allows for better results from LS-Factor. On the contrary, a coarse resolution showed generalized results that may lead to inadequate estimates of soil loss by applying the RUSLE model. Figures 3c, d show in better detail the incidence of DEMs scaling. Only in Andes Mountains the LS-Factor values were higher for the modified resolution of 4 km in relation to the original scale of 30 m, due to the increase that this processing generates in L-Factor. Therefore, an increase

in original scale generates more smoothed values of the LS-Factor at national scale.

LS Factor at a spatial resolution of 1 km (Fig. 3a) presented values between 0.03 and 124, and a mean value of 8.35, while at a spatial scale of 30 m (Fig. 3c) it showed consolidated values between 0.03 and 200, although isolated values over 5000 were recorded. However, their average value was less than 6.

LS-Factors analysis obtained from DEMs scaled to 4 km (Fig. 3b, d) presented very close results (between 0.03 and 103 for HydroSHEDS and between 0.03 and 113 for SRTM, both with a mean value close to 6).

**Influence of DEMs spatial resolution in LS-Factor at basin scale**

This section analyzes the effects of DEM spatial resolution of 3 different databases on the estimation of LS-Factor at a basin scale. Figure 4 allows for a more detailed analysis (ECB Portoviejo, ID 9) of the influence of spatial scale on LS-Factor. On this occasion, spatial resolution of 12.5 m of ALOS PALSAR (Fig. 4e) was added. Resolutions of 30 m (Fig. 4c) and 12.5 m (Fig. 4e) allow to correctly identify the drainage networks, which correspond very well to their topography, unlike the resolution of 1 km (Fig. 4a) that presents a much poorer detail, limiting the identification of relevant parameters of study area. At this level, very particular

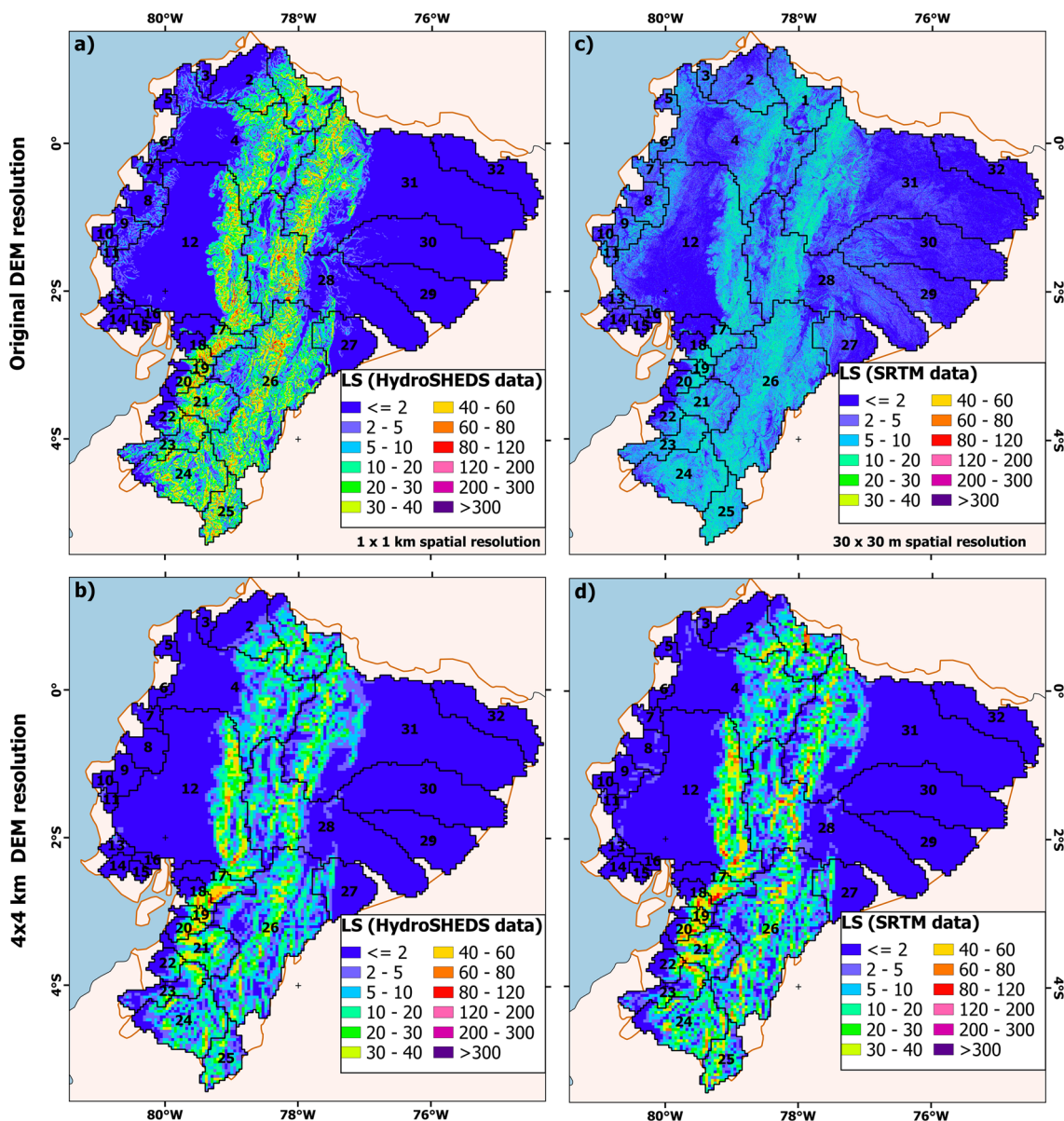


**Fig. 3** LS-Factor results for HydroSHEDS (a and b) and SRTM (c and d) databases. Details of the spatial resolution are seen to the left of each row

observations stand out. It would be expected that the finer resolution (12.5 m) would better estimate LS-Factor results, but this was not the case. This resolution had its limitations. When comparing areas close to the channel of the basin, it was observed that their widths could not be correctly estimated, because it estimates the channel networks as a line, this width being equal to the cell size (12.5 m), diluting even with the nearby areas (especially in the smaller branches).

When working with DEMs scaled to 4 km, it was observed that their original resolutions also influence the LS-Factor results, which could not be identified in the general scale of Fig. 3. Figure 4b, which was obtained from

scaling to an original resolution of 1 km, showed results limited to a single range (less than or equal to 2). When comparing Fig. 4b with Fig. 4d, e, it might be thought that the appearance of a few new pixels with another range of values may not be relevant, but if it is observed that these differences are being plotted only in a basin of 1905 m<sup>2</sup>, it could be expected that in the total study area at the national scale (approximately 230,000 km<sup>2</sup>), changes would be more considerable (although the mean values remain similar, a finer original resolution scaled to a higher spatial resolution may yield better estimates of soil loss using the RUSLE model).

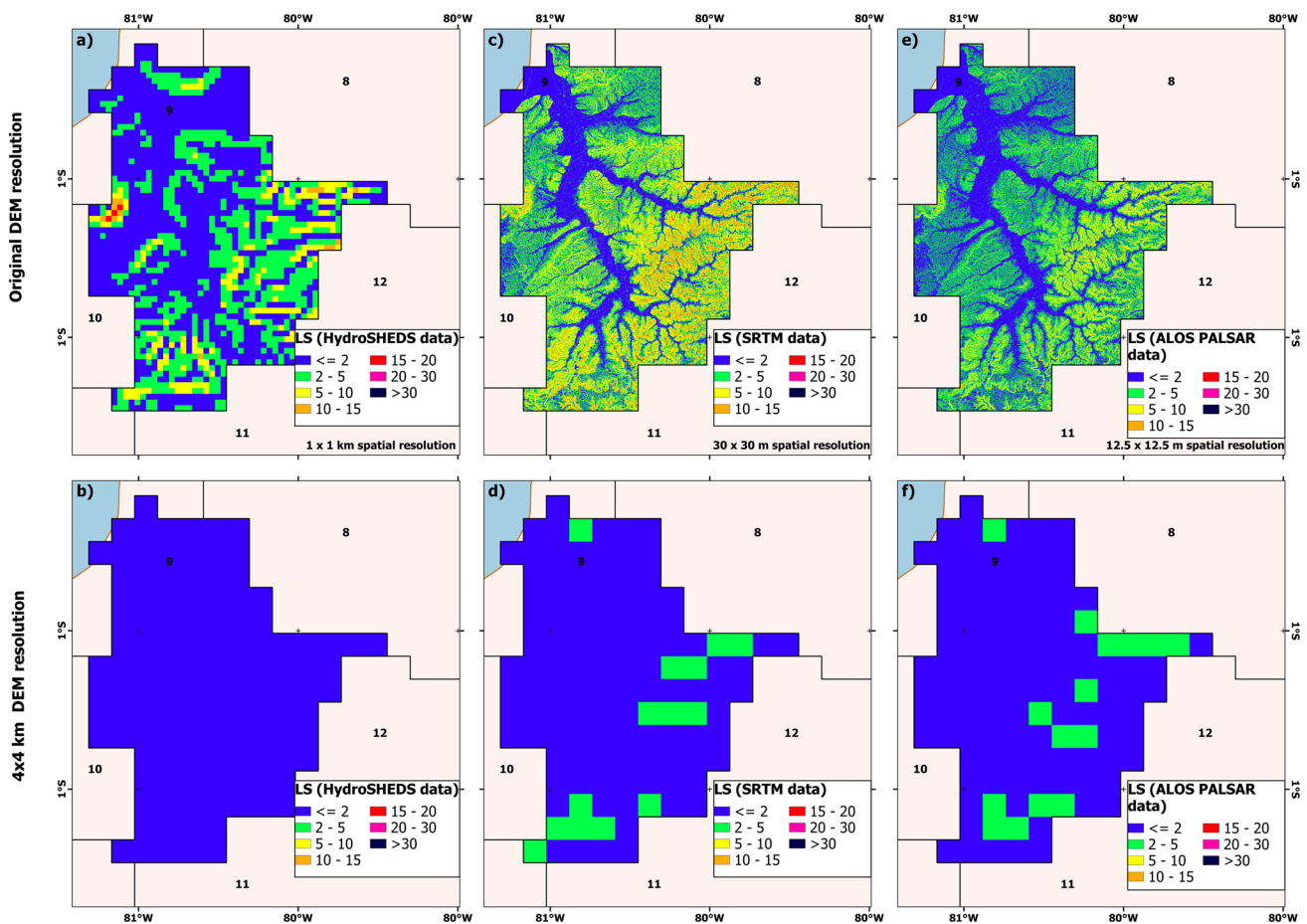


**Fig. 4** LS-Factor for HydroSHEDS (a and b), SRTM (c and d) and ALOS PALSAR (e and f) DEMs databases in ECB Portoviejo. Details of the spatial resolution are seen to the left of each row

Therefore, after the modification of the original resolutions of the DEM to a resolution of 4 km, ALOS PALSAR saved more information than its original resolution, although it was barely superior to SRTM (a finer scaled DEM will save more features when scaled to a coarser resolution). Nevertheless, knowing that ALOS PALSAR database presents limitations when calculating the LS-Factor and that the available information also does not cover the entire Ecuadorian territory, database that behaves best for calculating the LS-Factor is SRTM.

In Fig. 5, ECB Portoviejo (ID 9) and ATB Morona (ID 27) are analyzed at a spatial scale of 1 km, without considering ALOS PALSAR database (it does not cover part of ATB Morona). For ECB Portoviejo (Fig. 5a, b), it can be observed that the results of LS-Factor using SRTM scaled to 1 km maintains more information from its original DEM and the results are more detailed. For this basin, LS-Factor values ranged between 0.03 and 18.53 for HydroSHEDS, while for SRTM they ranged between 0.03 and 29.38. ATB Morona (Fig. 5c, d), which has very different characteristics from ECB Portoviejo, highlighting the presence of steeper slopes,

also presents differences in the pixels distribution when LS-Factor is calculated with HydroSHEDS and SRTM to 1 km, demonstrating again that the original scaling of SRTM maintains more information in relation to HydroSHEDS (data range varied between 0.03 and 59.58 for HydroSHEDS and; between 0.03 and 67.43 for SRTM). This makes it possible to identify that it is advisable to use a DEMs database with finer original scales and modify its dimensions to a coarser scale to improve the quality of the results.

**Statistical comparison of DEMs databases considering LS-Factor values**

LS-Factor analysis will be carried out at basin and pixel level, for resolutions of 1 and 4 km, using HydroSHEDS and SRTM databases (Fig. 6). At pixel level (Fig. 6a, c) better statistical approximations are obtained with resolutions modified on a larger scale (4 km in Fig. 6a;  $R^2 = 0.90$  and  $RMSE = 4.32$ ). This shows that, at a higher scale, the loss of detail in relation to finer resolutions is much greater. Both databases scaled to 4 km store very little

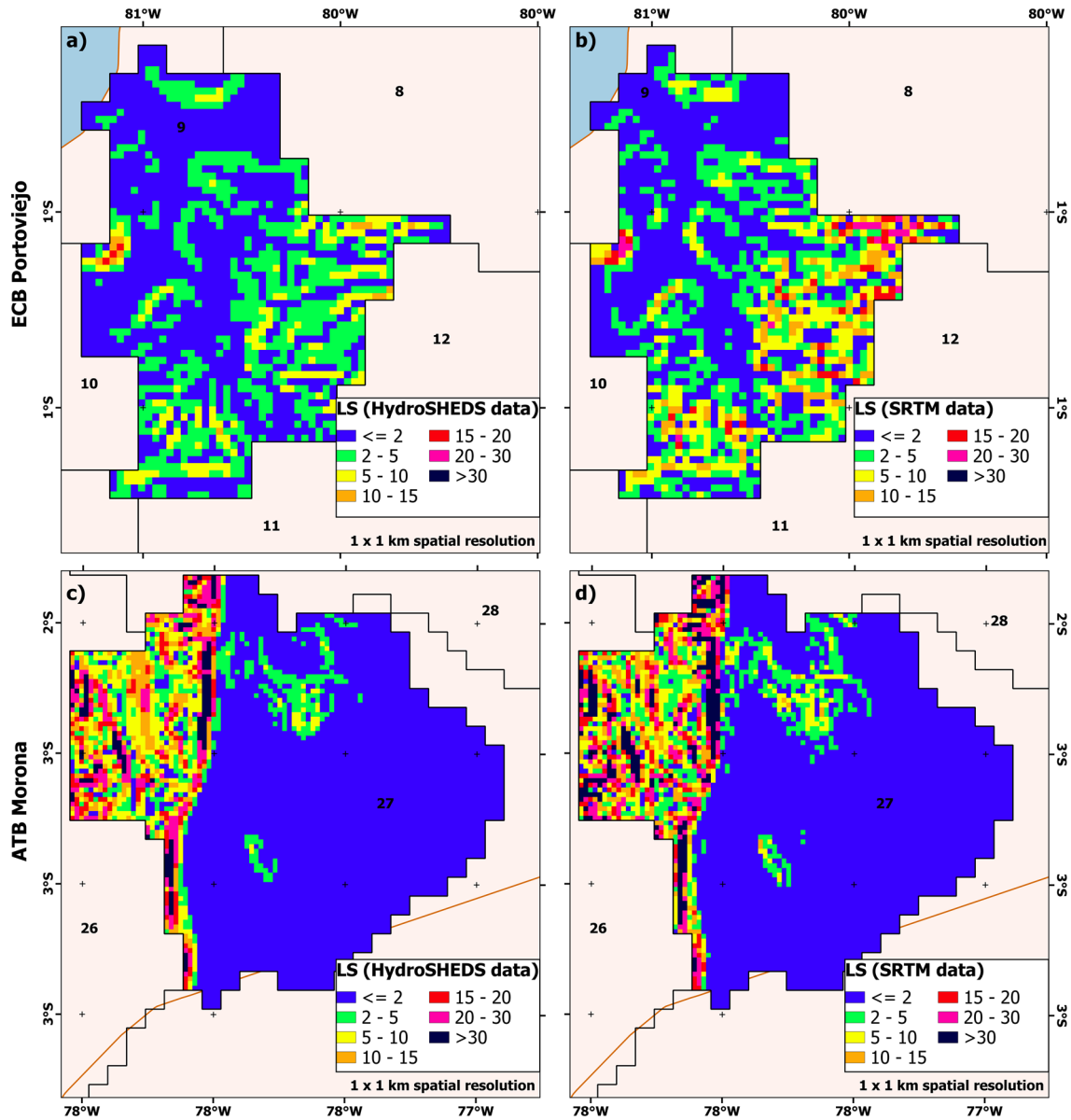


Fig. 5 LS-Factor for ECB Portoviejo HydroSHEDS (a) and SRTM (b); for ATB Morona HydroSHEDS (c) and SRTM (d). Basins are seen to the left of each row (plots scales are different to improve details)

information from their original DEMs, which generates a very similar LS-Factor distribution between both, obtaining acceptable correlations and squared errors. However, when matching SRTM database with that of HydroSHEDS at 1 km (Fig. 6c) even though there are still good statistical approximations ( $R^2 = 0.84$  and  $RMSE = 6.86$ ), results are clearly lower than those obtained with a larger scaling modification. This is because, as noted in previous sections, a finer original resolution will store more information when scaled to a coarser resolution, allowing SRTM results to be clearly better than those generated by HydroSHEDS. showing more visible changes in their

spatial distribution, thus generating a decrease in their statistical values at the time of comparison.

At basin level (Fig. 6b, d), statistical comparison is clearly less reliable, because it generates average values with less approximation (averages of large areas), moving away from a more precise and detailed analysis. Through this approach, both spatial scales registered a value of  $R^2 = 0.99$ , but through the RMSE it was possible to identify that the 4 km scale presented slightly more favorable statistical results (1.47 with reference to the 1.92 obtained with the scale of 1 km), obtaining conclusions like those described at the pixel scale.



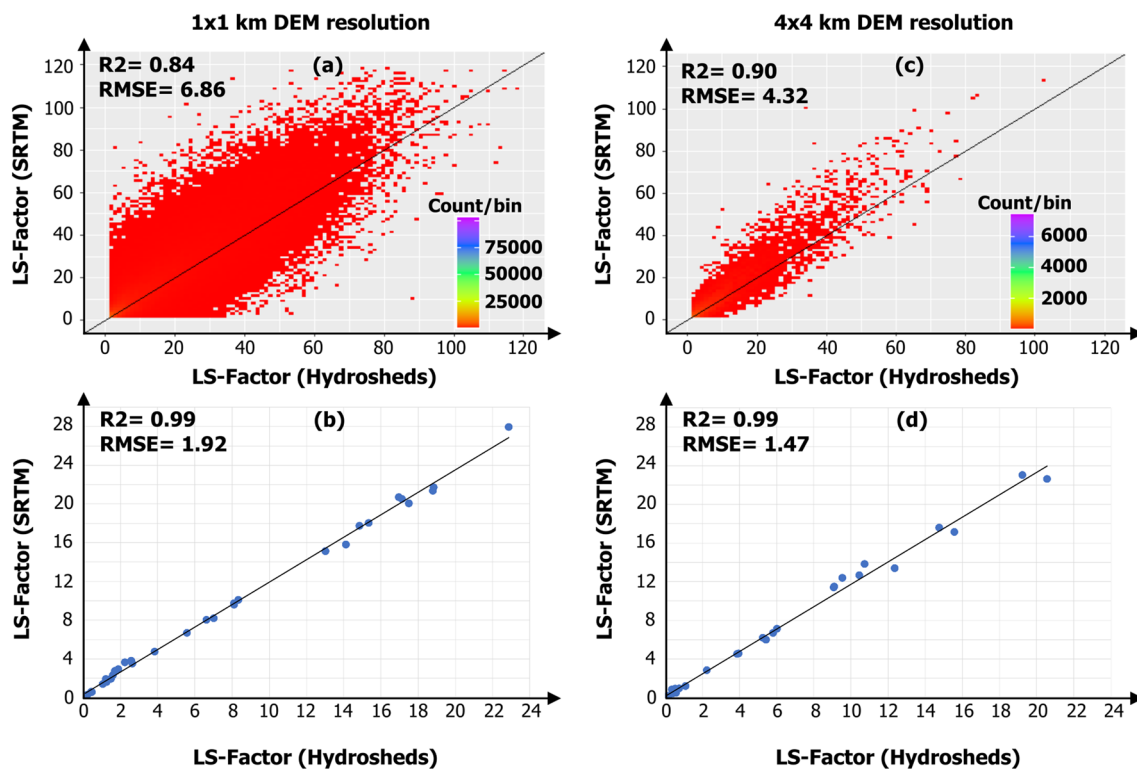


**Fig. 6** Scatterplot colored by density comparing LS-Factor values with 1 km (a) and 4 km (c) spatial resolution for SRTM and HydroSHEDS at pixel level. Scatterplot for 32 ECBs comparing LS-

Factor values at 1 km (b) and 4 km (d) spatial resolution for SRTM and HydroSHEDS. Black line is the identity line (1:1 line)

These results demonstrate that the original spatial scale used to perform the LS-Factor calculations has a strong impact on the range of results, and especially affects the “slopes” component (at a finer scale, the slopes ranged from  $0^{\circ}$  and  $88.89^{\circ}$ , while at a coarser scale the slopes ranged from  $0^{\circ}$  to  $15.2^{\circ}$ ).

### Alternative LS-Factor scaling process according to world literature

As it has been demonstrated in the previous sections, modifying the raster scale starting from a fine original database, allows to keep a greater amount of detail. Therefore, it is necessary to modify the resolution of each of the parameters that make up the LS-Factor before its calculation process (homogenize raster). However, there are procedures that apply different methodologies. Borelli et al. (2017), carry out a novel procedure in which, using the Desmet and Govers (1996) algorithm available in the SAGA module (present in QGIS and ArcGIS), they obtain the LS-Factor of an original scale of the SRTM DEM at 90 m. Subsequently, Borrelli et al. (2017) directly apply a scaling process to the LS-Factor obtained, to bring it to their analysis scale (250 m).

By analyzing Fig. 7 it can be seen that the difference between the combination of methodologies is evident.

Comparing the results of Fig. 7a with Fig. 7c, it can be seen that the results obtained underestimate the low values (generalize them) but better represent the high values (shown especially near the Andes Mountains). On the contrary, if the results of Fig. 7b are compared with Fig. 7c, it is evident that the low values are better represented by this procedure (calculation of the LS-Factor at original scale and subsequent scaling of the results to 4 km) but high results are underestimated (generalizes them). By analyzing Fig. 7d, the differences in the maximum values obtained from the results of each methodological process can be observed. Despite the fact that the Desmet & Govers (4 km) methodology allowed storing maximum values of 65 (considering that the maximum values obtained at the original scale of 90 m were greater than 350), the data median is much lower than the original scale (90 m) and the projected scale (90 m–4 km), which shows that the low results (which were underestimated) have a higher concentration in the Ecuadorian basins. On the other hand, the Demet & Govers procedure (90 m–4 km) maintains a data median very similar to that presented by the original scale, despite the fact that the maximum peaks are less than 26.

It is important to mention that, although it is true, the application of a scaling process to the elements that allow obtaining the LS-Factor before the calculation process is

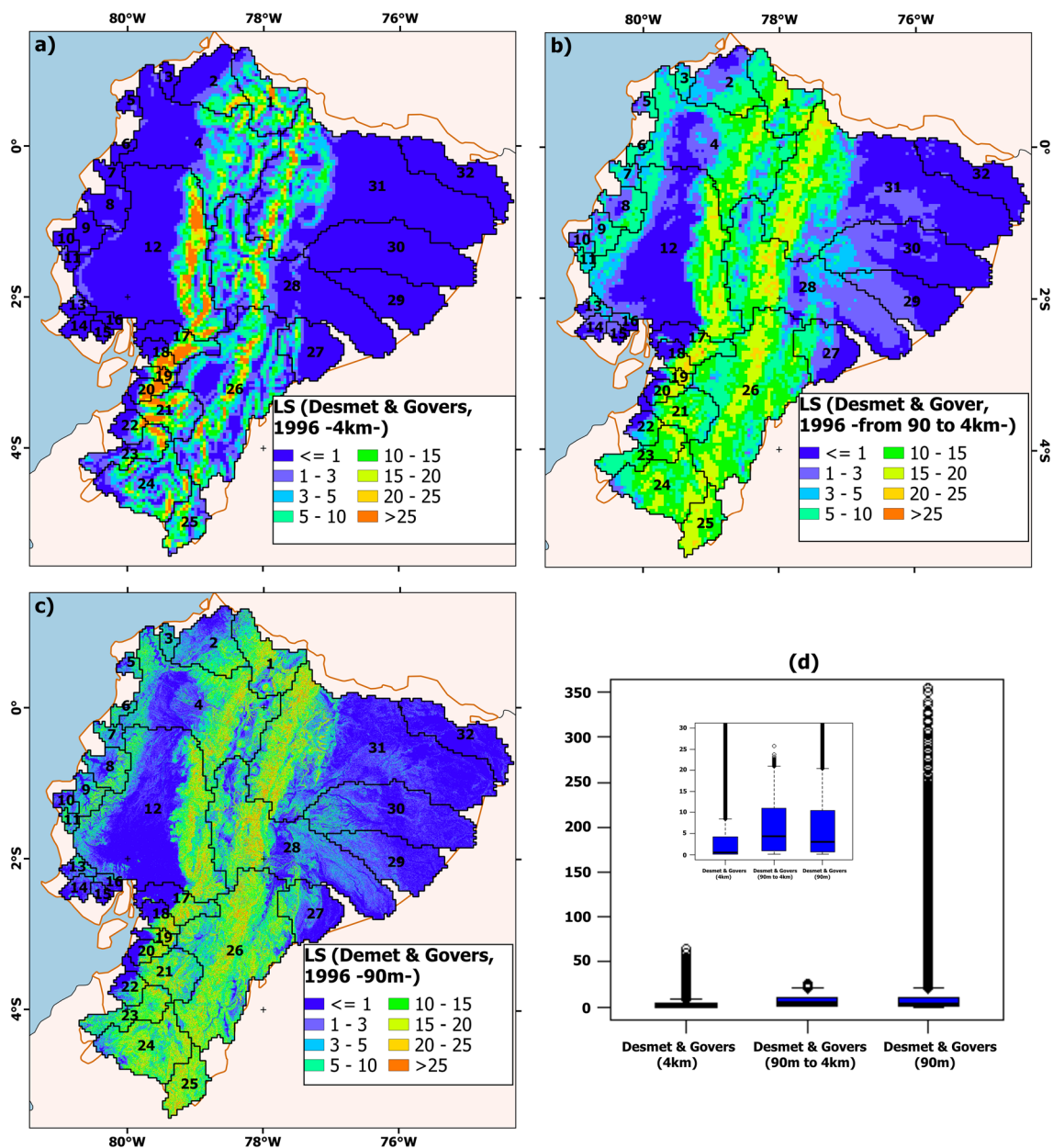


**Fig. 7** Analysis of the scaling procedure proposed by Borrelli et al. (2017) based on the SRTM database. **a** Calculation of the LS-Factor by means of the initial scaling of the DEM to 4 km and the subsequent application of the SAGA module. **b** Calculation of the LS-Factor by applying the SAGA module to the original 90 m DEM and its

subsequent scaling to 4 km. **c** LS-Factor calculated with the SAGA module at an original scale of 90 m. **d** Boxplot to compare the scale of values between the 3 previous processes (inner box shows a close-up of the results)

much more efficient (maintaining more information after the pixel size change) by means of application of Desmet and Govers (1996) for the individual calculation of L-Factor and the approach of Renard et al. (1996) based on McCool et al. (1987) for the individual calculation of the S-Factor, maintains high values (for the conditions of the Ecuadorian territory) that possibly should be eliminated when generating the erosion rates through the RUSLE approach. Regarding the simplified and automated calculation process of SAGA

(Desmet and Govers 1996) used directly to obtain the LS-Factor and its subsequent scaling to a spatial resolution of study, it can be very useful in particular situations, in addition to being fast and simple to apply.

It is recommended to apply the conventional scaling procedure before the calculation process for sectors where the elevations and slopes are less pronounced (more homogeneous), due to the better representation of the results (and the less appearance of pixels with offset values). On the other

hand, for areas similar to those of Ecuador (where the presence of the Andes Mountains conditions the topography of the landscape and generates very high values), the simplified methodology can also be useful, since it mainly eliminates the pixels with more distant values and that can generate results outside the normal ranges of soil erosion when applying the RUSLE model.

## Conclusions

The distribution of the LS-Factor and the sensitivity of DEMs spatial resolution in the calculation of their magnitudes at the national scale in Ecuador were evaluated for the first time. The gradient of the slope was the factor with the greatest influence on the LS-Factor results, identifying greater magnitudes in the Andes Mountains and in certain sections of the ECBs close to the Pacific Ocean (location of small coastal mountains). The influence of DEMs spatial resolution in the LS-Factor calculation showed very interesting and contrasting results. Finer resolutions made it possible to correctly identify the drainage networks, which correspond very well to their topography. At national scale, finer resolution of SRTM (30 m) showed much more reliable results relative to the coarser scale of the HydroSHEDS (1 km). At basin scale, it was expected that a finer resolution also presents better approximations of the LS-Factor. However, the finest resolution of analysis at basin level, which corresponds to ALOS PALSAR DEMs (12.5 m), presented limitations in their estimates. This finer resolution generated problems when estimating the channel widths of the basins, especially in the secondary branches, diluting results with the surrounding pixels. The statistical approaches allowed to identify a better linear agreement and a lower error of the satellite estimates between SRTM and HydroSHEDS when these were modified to a common scale of 4 km ( $R^2=0.90$ ; RMSE=4.32) in relation to a scaling of 1 km ( $R^2=0.84$ ; RMSE=6.86) at a per-pixel level. It was determined that SRTM DEMs database (30 m) was the most adequate to estimate the LS-Factor, allowing to obtain better approximations of soil erosion rates through the application of the RUSLE model. Even when its spatial resolutions are modified to a larger scale (4 km), SRTM was shown to hold more information compared to HydroSHEDS. As an alternative methodology, the calculation of the LS-Factor at an original scale of 90 m using the SAGA algorithm (Desmet & Govers 1996) and its subsequent scaling to the spatial resolution of the study (4 km) can be very useful for particular study areas such as Ecuador, where the topography is conditioned by the presence of the Andes Mountains. This alternative methodology was shown to correctly represent low values and eliminate high values that are out of phase. These results make it possible to improve the spatial models of soil loss

due to rainfall erosion, establishing more appropriate measures for water and soil conservation and management, disaster control, agricultural protection, and other applications in Ecuador.

**Acknowledgements** Authors thank the FSPI—Doctoral Schools Project of the French Embassy in Ecuador, funded by the Ministry of Europe and Foreign Affairs.

**Author contributions** All authors worked equally in the preparation of the manuscript.

**Funding** The authors have not disclosed any funding.

**Data availability** Data will be made available on request.

## Declarations

**Competing interests** The authors declare no competing interests.

## References

- Batista PV, Davies J, Silva ML, Quinton JN (2019) On the evaluation of soil erosion models: Are we doing enough? *Earth Sci Rev* 197:102898. <https://doi.org/10.1016/j.earscirev.2019.102898>
- Borrelli P, Robinson DA, Fleischer LR, Lugato E, Ballabio C, Alewell C, Panagos P (2017) An assessment of the global impact of 21st century land use change on soil erosion. *Nat Commun* 8(1):1–13. <https://doi.org/10.1038/s41467-017-02142-7>
- Borrelli P, Alewell C, Alvarez P, Anache JAA, Baartman J, Ballabio C, Panagos P (2021) Soil erosion modelling: A global review and statistical analysis. *Science of the total environment*, 780: 146494. <https://doi.org/10.1016/j.scitotenv.2021.146494>
- De Noni G, Asseline J, Viennot M (2000) Erosion des sols volcaniques de la cordillère des Andes, en Equateur. *Revue De Géographie Alpine* 88(2):13–26
- Delgado D, Sadaoui M, Ludwig W, Méndez W (2022) Spatio-temporal assessment of rainfall erosivity in Ecuador based on RUSLE using satellite-based high frequency GPM-IMERG precipitation data. *CATENA* 219:106597. <https://doi.org/10.1016/j.catena.2022.106597>
- Delgado D, Sadaoui M, Ludwig W, Mendez W (2023) Depth of the pedological profile as a conditioning factor of soil erodibility (RUSLE K-Factor) in Ecuadorian basins. *Environ Earth Sci* 82(12):286. <https://doi.org/10.1007/s12665-023-10944-w>
- Delgado D, Sadaoui M, Pacheco H, Méndez W, Ludwig W (2021) Interrelations between soil erosion conditioning factors in basins of Ecuador: contributions to the spatial model construction. In: *Proceedings of the 1st international conference on water energy food and sustainability (ICoWEFS 2021)*. ICoWEFS 2021. Springer, Cham. [https://doi.org/10.1007/978-3-030-75315-3\\_94](https://doi.org/10.1007/978-3-030-75315-3_94)
- Desmet P, Govers G (1996) A GIS procedure for automatically calculating the USLE LS factor on topographically complex landscape units. *J Soil Water Conserv* 51:427–433
- Earth Resources Observation and Science Center (EROS). (2017). Shuttle Radar Topography Mission (SRTM) 1 Arc-Second Global . U.S. Geological Survey. <https://doi.org/10.5066/F7PR7TFT>
- Elnashar A, Zeng H, Wu B, Fenta AA, Nabil M, Duerler R (2021) Soil erosion assessment in the Blue Nile Basin driven by a novel RUSLE-GEE framework. *Sci Total Environ* 793:148466. <https://doi.org/10.1016/j.scitotenv.2021.148466>

- Environmental Systems Research Institute (ESRI). (1992). ArcWorld, 1:3M, Redlands, Calif.
- Environmental Systems Research Institute (ESRI). (1993). Digital chart of the world, 1:1M, Red-lands, Calif.
- Harden CP (2001) Soil erosion and sustainable mountain development. *Mt Res Dev* 21(1):77–83. [https://doi.org/10.1659/0276-4741\(2001\)021\[0077:SEASMD\]2.0.CO;2](https://doi.org/10.1659/0276-4741(2001)021[0077:SEASMD]2.0.CO;2)
- Harden C (1988) Mesoscale estimation of soil erosion in the Rio Ambato drainage, Ecuadorian Sierra. *Mountain Research and Development*, 331–341. <https://doi.org/10.2307/3673556>
- Lehner B, Verdin K, Jarvis A (2008) New global hydrography derived from spaceborne elevation data. *EOS Trans Am Geophys Union* 89(10):93–94. <https://doi.org/10.1029/2008EO100001>
- Li K, Wang L, Wang Z, Hu Y, Zeng Y, Yan H, Shi Z (2022) Multiple perspective accountings of cropland soil erosion in China reveal its complex connection with socioeconomic activities. *Agriculture, Ecosyst Environ* 337:108083. <https://doi.org/10.1016/j.agee.2022.108083>
- McCool DK, Brown LC, Foster GR, Mutchler CK, Meyer LD (1987) Revised slope steepness factor for the Universal Soil Loss Equation. *Transactions of the ASAE* 30(5):1387–1396
- Melkam, E. (2003). *Crop Land Soil Erosion Prediction Using WEEP Model*.
- Mendoza EFM, Arteaga EAG, Delgado D (2023) La erosividad de la lluvia como factor condicionante de la erosión hídrica en Manabí. *Polo Del Conocimiento* 8(2):68–81
- Molina A, Govers G, Vanacker V, Poesen J, Zeelmaekers E, Cisneros F (2007) Runoff generation in a degraded Andean ecosystem: Interaction of vegetation cover and land use. *CATENA* 71(2):357–370. <https://doi.org/10.1016/j.catena.2007.04.002>
- Molnar D, Julien P (1998) Estimation of upland erosion using GIS. *Comput Geosci* 24:183–192
- Montanarella L, Badraoui M, Chude V, Costa IDSB, Mamo T, Yemefack M, McKenzie N (2015) Status of the world's soil resources: main report. Embrapa Solos-Livro científico (ALICE). <http://www.alice.cnptia.embrapa.br/alice/handle/doc/1034770>
- Mukherjee S, Joshi PK, Mukherjee S, Ghosh A, Garg RD, Mukhopadhyay A (2014) Evaluation of vertical accuracy of open source Digital Elevation Model (DEM). *Int J Appl Earth Observ Geoinf* 21:205–217. <https://doi.org/10.1016/j.jag.2012.09.004>
- Ochoa-Cueva P, Fries A, Montesinos P, Rodríguez-Díaz JA, Boll J (2015) Spatial estimation of soil erosion risk by land-cover change in the andes of southern Ecuador. *L Degrad Dev* 26:565–573. <https://doi.org/10.1002/ldr.2219>
- Pacheco HA, Méndez W, Moro A (2019) Soil erosion risk zoning in the Ecuadorian coastal region using geo-technological tools. *Earth Sci Res J* 23(4):293–302. <https://doi.org/10.15446/esrj.v23n4.71706>
- Panagos P, Borrelli P, Meusburger K (2015) A new European slope length and steepness factor (LS-Factor) for modeling soil erosion by water. *Geosciences* 5(2):117–126. <https://doi.org/10.3390/geosciences5020117>
- Panagos P, Ballabio C, Himics M, Scarpa S, Matthews F, Bogonos M, Borrelli P (2021) Projections of soil loss by water erosion in Europe by 2050. *Environ Sci Policy* 124:380–392. <https://doi.org/10.1016/j.envsci.2021.07.012>
- Párraga AJF, Tejena ÁAR, Gutiérrez DAD (2023) Análisis de la distribución espacial de la erodabilidad del suelo en la cuenca del Río Esmeraldas-Ecuador. *Polo Del Conocimiento* 8(2):82–95
- Renard KG, Laflen JM, Foster GR, McCool DK (1991) The revised universal soil loss equation. In *Soil erosion research methods* (pp. 105–126). Routledge.
- Renard KG, Foster GR, Weesies GA, McCool DK, Yoder DC (1996) Predicting soil erosion by water: A guide to conservation planning with the Revised Universal Soil Loss Equation (RUSLE). *Agriculture handbook*, 703.
- Reyes P (2013) *Évolution du relief le long des marges actives: étude de la déformation Plio-Quaternaire de la cordillère côtière d'Équateur* (Doctoral dissertation, Université Nice Sophia Antipolis).
- Senanayake S, Pradhan B, Alamri A, Park HJ (2022) A new application of deep neural network (LSTM) and RUSLE models in soil erosion prediction. *Sci Total Environ* 845:157220. <https://doi.org/10.1016/j.scitotenv.2022.157220>
- Thomas J, Joseph S, Thirivikramji KP (2018) Assessment of soil erosion in a tropical mountain river basin of the southern Western Ghats, India using RUSLE and GIS. *Geosci Front* 9(3):893–906. <https://doi.org/10.1016/j.gsf.2017.05.011>
- Vanacker V, von Blanckenburg F, Govers G, Molina A, Poesen J, Deckers J, Kubik P (2007) Restoring dense vegetation can slow mountain erosion to near natural benchmark levels. *Geology* 35(4):303–306. <https://doi.org/10.1130/G23109A.1>
- Vanacker V, Molina A, Rosas MA, Bonnesoeur V, Román-Dañobeytia F, Ochoa-Tocachi BF, Buytaert W (2022) The effect of natural infrastructure on water erosion mitigation in the Andes. *Soil* 8(1):133–147. <https://doi.org/10.5194/soil-8-133-2022>
- Véliz MAM, Guillen PAF, Delgado D (2023) Evaluación espacio-temporal del factor C de la Rusle entre las cuencas del río Portoviejo y Chone. *Domino De Las Ciencias* 9(3):1300–1315

**Publisher's Note** Springer Nature remains neutral with regard to jurisdictional claims in published maps and institutional affiliations.

Springer Nature or its licensor (e.g. a society or other partner) holds exclusive rights to this article under a publishing agreement with the author(s) or other rightsholder(s); author self-archiving of the accepted manuscript version of this article is solely governed by the terms of such publishing agreement and applicable law.